Measuring endocytosis during proliferative cell quiescence

Claudia Hinze [1,2], Kieran McGourty[1,3] and Emmanuel Boucrot[1,4,*]

[1] Institute of Structural and Molecular Biology, University College London, Gower Street, London WC1E 6BT, UK
[2] Present address: Institute of Immunity and Transplantation, Division of Infection and Immunity, University College London, Royal Free Campus, NW3 2PF London, UK
[3] Present address: Department of Chemical Sciences, Bernal Institute and Health Research Institute, University of Limerick, IRL
[4] Institute of Structural and Molecular Biology, Birkbeck College, Malet Street, London WC1E 7HX, UK
*Correspondence: e.boucrot@ucl.ac.uk

Abstract

Quiescence (also called the 'G0') is the state in which cells have exited the cell cycle but are capable to re-enter as required. Though poorly understood, it represents one of the most prevalent cell states across all life. Many biologically important cell types reside in quiescence including mature hepatocytes, endothelial cells and dormant adult stem cells. Furthermore, the quiescence program occurs in both short-and long-term varieties, depending on the physiological environments. A barrier slowing our understanding of quiescence has been a scarcity of available *in vitro* model systems to allow for the exploration of key regulatory pathways, such as endocytosis. Endocytosis, the internalization of extracellular material into the cell, is a fundamental and highly regulated process that impacts many cell-biological functions. Accordingly, we have developed an *in vitro* model of deep quiescence in hTERT-immortalized RPE1 cells, combining both long-term contact inhibition and mitogen removal, to measure endocytosis. In addition, we present an analytical approach employing automated high-throughput microscopy and image analysis that yields high content data allowing for meaningful and statically robust interpretation. Importantly, the methods presented herein provide a suitable platform that can be easily adapted to investigate other regulatory processes across the proliferative cell cycle.

Key words: Cell cycle, cell quiescence, G0, primary cells, hTERT-immortalized cells, endocytosis, clathrin-mediated endocytosis, macropinocytosis, fluid-phase uptake, epidermal growth factor, automated high-throughput microscopy, high-throughput image analysis.

1. Introduction

Cell quiescence is the most common cell state amongst all cellular organisms and is defined as a temporary and reversible absence from proliferation (Daignan-Fornier and Sagot 2011). This is different from senescence or terminal cell differentiation, which are irreversible exits from the cell cycle. Quiescent cells, such as most adult stem cells, are actively maintained in a quiescent state but can re-enter the cell cycle when stimulated to rapidly expand and differentiate, enabling efficient tissue homeostasis. As such, quiescence is a

default state that cells revert to when faced with a challenge to proliferation such as a lack of nutrients, mitogen signaling or space (contact inhibition) (Fuge et al. 1994; Herman 2002; Gos et al. 2005; Coller et al. 2006; Lemons et al. 2010). It is also a mechanism for cells to preserve their function over a long period of time. Quiescent cells are defined by having a diploid ('2N') genome (Gray et al. 2004), low levels of cell cycle markers (*e.g.,* Ki67, nuclear CyclinD1 or phosphorylated Retinoblastoma protein), high levels of cyclin-dependent kinase inhibitors $p21^{Cip1}$ and $p27^{Kip1}$ (Coller et al. 2006; Gookin et al. 2017), elevated autophagy activity (Valentin and Yang 2008) and decreased levels and translation of mRNA (Crissman et al. 1985; Fuge et al. 1994). As well as having a smaller cell size and an increased volume ratio of nucleus to cytoplasm (Yusuf and Fruman 2003; Coller et al. 2006; Lemons et al. 2010). The traditional understanding of cell quiescence was that the cell was completely dormant and stagnant (*e.g.* the 'sleeping beauty' state in Baker's yeast (Gray et al. 2004). As more research has been carried out on proliferative quiescence, new evidence showed that this cell state is dynamic and actively maintained by a specific cellular transcriptional, signaling and metabolic program. Despite the prevalence non-dividing quiescent cells in the body, quiescence is relatively understudied, and little is understood about the signaling mechanisms that govern it. Studies have found that upon entry into quiescence, the cell undergoes a reorganization of its cellular structure. The actin cytoskeleton is relocated into actin bodies (Sagot et al. 2006); yeast relocates its proteasome from the nucleus into storage chambers in the cytoplasm (Laporte et al. 2008) and many cytoplasmic proteins are compartmentalized into molecular complexes (Narayanaswamy et al. 2009).

There are several *in vitro* culture systems of quiescence that use (combinations of or in isolation): contact inhibition, mitogen deprivation, nutrient starvation or loss of adhesion (Benecke et al. 1978; Gos et al. 2005; Coller et al. 2006; Lemons et al. 2010; Wang et al. 2017). Though each approach allows cell cycle exit, they induce different cellular programs such as mechanotransduction regulatory mechanism after contact inhibition or mitogen-dependent reduction in proliferation signaling cascades during mitogen removal (Gos et al. 2005; Coller et al. 2006; Lemons et al. 2010; Gookin et al. 2017; Wang et al. 2017). Interestingly, cell model systems that relied on varying the duration of contact inhibition resulted in the generation of heterogenous populations of both deep and shallow quiescent cells - with increased length being correlated with increased depth of quiescence (Augenlicht and Baserga 1974; Owen et al. 1989; Yanez and O'Farrell 1989; Soprano 1994; Coller et al. 2006; Lemons et al. 2010; Gookin et al. 2017; Wang et al. 2017). Similarly, the duration of reduced mitogen correlated with the depth of the quiescent program (Lemons et al. 2010; Gookin et al. 2017; Wang et al. 2017). Another source of heterogeneity is the variability in cell samples. As regular cell lines are usually of tumor origin, they lost contact inhibition and/or sensitivity to mitogen removal and do not enter G0 (Hanahan and Weinberg 2011). Primary cells are commonly used instead, but as they enter replicative senescence after few passages *in vitro* (Sherr and DePinho 2000), new cell samples are required regularly. Because of the genetic diversity of the cell donors, it typically leads to heterogeneity in the experiments. These limitations can be overcome by the use of cells immortalized by the human telomerase reverse transcriptase (hTERT). Such cell lines retain primary characteristics for several hundreds of passages *in vitro*, allowing for the reproducibility of experiments over long periods of time (Bodnar et al. 1998; Kogan et al. 2006). There are now hTERT-immortalized cells from 16 human tissues available commercially.

Accordingly, we have generated a quiescent cell culture model that use hTERT-immortalized cell lines in combination to both long duration contact-inhibition and an extended period of mitogen removal. This approach has yielded a reproducible and largely homogenous cell culture system with characteristics of long-term quiescence. Here, we employ this culture model to measure endocytosis during deep quiescence.

Endocytosis is the process by which cells acquire substances from outside the cell and internalize surface membrane proteins (Doherty and McMahon 2009). Endocytosis is required by all eukaryotic cells for communication with their environment, internalization of micronutrients and for turnover of cell surface components. It not only supports the steady state distribution of cell surface receptors but also regulates their activity by mediating their removal from the cell surface and degradation by lysosomes. As such, endocytosis plays key roles in biological processed such as synaptic transmission, signal transduction and in controlling developmental processes regulating cell fate (Sigismund et al. 2012; Sigismund and Scita 2018; Hinze and Boucrot 2018). The process occurs through invaginations on the plasma membrane forming endocytic vesicles that carry the 'cargo' molecules (nutrient or receptors). The detachment of endocytic carriers relies on the GTPase Dynamin or other scission mechanisms (Renard et al. 2018). Furthermore, endocytosis is also exploited by many pathogens (toxins, viruses, bacteria) as portal of entry. Mis-regulation of endocytosis through mutation or other means can cause a broad range of diseases including cancer, atherosclerosis, neurodegeneration, and lysosomal storage diseases (McMahon and Boucrot 2011; Sigismund et al. 2012; Schmid 2017).

There are several parallel endocytic pathways. The most thoroughly described of them is Clathrin-mediated endocytosis (CME), which is the dominant uptake mechanism supporting cellular homeostasis (Mettlen et al. 2018; Kaksonen and Roux 2018). This constitutive process has a molecular hallmark attributed to the dependency on Clathrin, a triskelion-shaped scaffold protein comprising three light and three heavy chains (Mettlen et al. 2018; Kaksonen and Roux 2018). Cells also contain several clathrin-independent pathways of endocytosis (CIE) that allow them to take up membrane and extracellular components in diverse geometries at both macro and micro scales (Ferreira and Boucrot 2018; Hemalatha and Mayor 2019). Generally, CIE are involved in cellular processes outside of a housekeeping role, including rapid removal of activated receptors for the plasma membrane, bulk lipid or protein internalization and cell morphology events like migration, polarization and cell spreading (Ferreira and Boucrot 2018; Hemalatha and Mayor 2019). CIE pathways can be further subdivided by the scales and morphology of the membrane cargo carriers that they internalize, including large (0.2 to >10 μm) membrane macropinosomes, tubular carriers as occurs in activated pathways like fast-endophilin-mediated-endocytosis (FEME) and small (50-200 nm) micropinosomes such as CLIC/GEEC (Ferreira and Boucrot 2018). Each of these separate CIE pathways are further segregated by their dependency on dynamin and the cargos they transport (Maldonado-Báez et al. 2013; Ferreira and Boucrot 2018; Hemalatha and Mayor 2019).

Given the fundamental nature of endocytosis and the breath of the biological processes that it mediates, it is expected that its activity varies along the cell cycle, including quiescence. However, evidence to date is biased towards permanently proliferating cells as the vast majority of studies used cancer cell lines that cannot enter quiescence (Hanahan and Weinberg 2011). Here, we present a high-throughput imaging approach, coupled to open-source automated image analysis, that allows for the analysis of various endocytic pathways in both actively cycling cell populations and in long-term quiescent populations. The approach ensures that each stage of the cell cycle is represented with sufficient cell numbers (many thousands) to allow for robust statistical analysis. Lastly, the cellular models and analysis approaches presented are readily suitable to be adapted to other cellular events beyond endocytosis that may vary across the full spectrum of the proliferative cell cycle.

2. Materials

1. Primary cells (*e.g.* primary fibroblasts, HUVEC) or hTERT-immortalized normal cells (*e.g.* RPE1) (*see* **Note 1**).
2. Serum-containing culture medium appropriated for cells used in 2.1. (*see* **Note 2**).
3. Serum-free culture medium appropriated for cells used in 2.1. (*see* **Note 3**).
4. Enzyme-free cell detachment solution (*e.g.* S-014-B, Millipore) (*see* **Note 4**).
5. CASY Cell Counter and Analyzer Model TT (Roche Applied Science) or equivalent.
6. Glass- or cycloolefin-bottom 96-well microplates (*e.g.* 655892, Greiner Bio-One) (*see* **Note 5**).
7. Phosphate-buffered saline (PBS) buffer: 137 mM NaCl, 2.7 mM KCl, 12.5 mM Na_2HPO_4, 2 mM KH_2PO_4 equilibrated at pH 7.4.
8. PBS^{++}: containing 0.9 mM $CaCl_2$ and 0.5 mM $MgCl_2$ (*see* **Note 6**).
9. Treatments being investigated (inhibitor drugs, siRNA, plasmids etc.). Here, we provide guidance for the use of chemical inhibitors blocking CME (Pitstop 2, stock 50 mM in DMSO; *see* **Note 7**), Dynamin-dependent endocytosis (Dyngo-4a, stock 30 mM in DMSO, Chlorpromazine stock 20 mM in water (*see* **Note 8**); Dynole 34-2 stock 10 mM in DMSO; Indole 24 stock 30 mM in DMSO; Quinone 45 stock 30 mM in DMSO; Pyrimidyn 7, stock 30 mM in DMSO; MitMAB, stock 10 mM in water; Aminopyrimidine, stock 20 mM in DMSO, or Dynasore, stock 50 mM in DMSO) and macropinocytosis (EIPA, stock 50 mM in DMSO; Rottlerin, stock 5 mM in DMSO) as well as RNA interference of AP2 (siRNA oligonucleotides (CCGCCAGAUGGAGAGUUUGAGCUUA and UAAGCUCAAACUCUCCAUCUGGCGG, Dharmacon) reconstituted in miliQ water to a 20μM stock. (*see* **Note 9**).
10. Transfection reagent as appropriate for the cell type used (*e.g.* Lipofectamine RNAiMAX, Thermo Scientific).
11. OptiMEM medium (Thermo Scientific), used to form RNAi-Lipofectamine complexes.
12. Fluorescently-labelled ligands to monitor CME (*e.g.* AlexaFluor488-, AlexaFluor555- or AlexaFluor647-labelled Transferrin; all Thermo Scientific and DiI- or DiO-labelled Low density Lipoprotein (LDL); LifeTech or Kalen Biomedical), Dynamin-dependent endocytosis (*e.g.* AlexaFluor488-, AlexaFluor555- or AlexaFluor647-labelled Epidermal Growth Factor (EGF); all Thermo Scientific) and macroinocytosis (*e.g.* AlexaFluor555-, AlexaFluor647- or TRITC-labelled Dextran of various sizes (3,000 to 70,000 kDa), Lucifer yellow, DQ Green BSA, all Thermo Scientific). (*see* **Note 10**).
13. Antibodies suitable for endocytic feeding assays (e.g. anti-TfR or anti-EGFR antibody). (*see* **Note 11**).
14. Ligand Uptake Assay (LUA) medium: regular serum-free or full growth medium or α-MEM without phenol red (Thermo Scientific) supplemented with 20 mM Hepes (Sigma), pH 7.2 and 1% BSA (Sigma).
15. Stripping Buffer 1 (pH 5.5): 150mM NaCl, 100mM Glycine, 5mM KCl, 1mM $CaCl_2$, 1mM $MgCl_2$ adjusted to pH5.5.
16. Stripping Buffer 2 (pH 2): 150 mM NaCl, 0.2M acetic acid, 5mM KCl, 1mM $CaCl_2$, 1mM $MgCl_2$, adjusted to pH2.
17. Paraformaldehyde (PFA), diluted to 4% in PBS.
18. PBS containing 50 mM NH_4Cl.
19. Hoechstt 33342 (stock 10 mg/mL in water) and DAPI (stock 1 mg/mL in water) (*see* **Note 12**).
20. Fluorescent microscope. Here we describe a procedure using an ImageXpress Micro XL Widefield High Content Screening System (Molecular Devices) equipped with Nikon ELWD 20X or 40X S Plan Fluor air objective (numerical aperture = 0.45) and an environmental temperature and CO2 control module, Lumencor Sola solid-state white-light engine with wavelengths ranging from 380 to 670 nm, band-pass filter cubes and 4.66 megapixel complementary metal-oxide semiconductor (CMOS) camera acquiring images

as 16 bit grayscale images at 2160 x 2160 pixels with one image per acquired channel and controlled by the MetaXpress 5.3 software (*see* **Note 13**).

21. Saponin (Sigma).

22. Microscopy slide mounting solution (Mowiol or equivalent), containing antifading agent (DABCO or equivalent).

3. Methods

3.1. Maintenance of exponentially growing cells

1. Grow cells in full-medium at 37 ℃.

2. Passage cells when they reach ~70% confluency (*see* **Note 14**).

2.1. Detach cells using non-enzymatic cell detachment solution (10 min, 37 ℃)(*see* **Note 4**).

2.2. Seed cells at 0.75 to 1.5 x 10^4 cells/cm^2 (or 1:10 to 1:5 volume dilution ratio) (*see* **Note 15**)

3. Change medium every 2 days. (*see* **Note 16**)

4. Two days before experiments, growing cells were seeded in the appropriated dish or plate format at a density of 1.5 x 10^4 cells/cm^2.

3.2. Induction of cellular quiescence

1. Use exponentially growing cell cultures at ~70% confluency (*see* **Note 14**).

2. Detach cells using enzyme-free cell detachment solution (10 min, 37 ℃)(*see* **Note 4**).

3. Count cells and seed them in the appropriated dish or plate format at a density of 1.4 x 10^4 cells/cm^2 (*see* **Note 17**).

4. Change medium (full serum) every 2 days. (*see* **Note 18**).

5. Grow cells in full medium for at least 7 days until they reach confluence and form a homogeneous monolayer (*see* **Note 19**).

6. Change medium to growth factor-free (serum-free) medium (*see* **Note 20**)

7. Change medium (serum-free) every 2 days.

8. Maintain cells for at least 10 days (at least 17 days from seeding) to induce deep quiescence (**Figure 1)** (*see* **Note 21**).

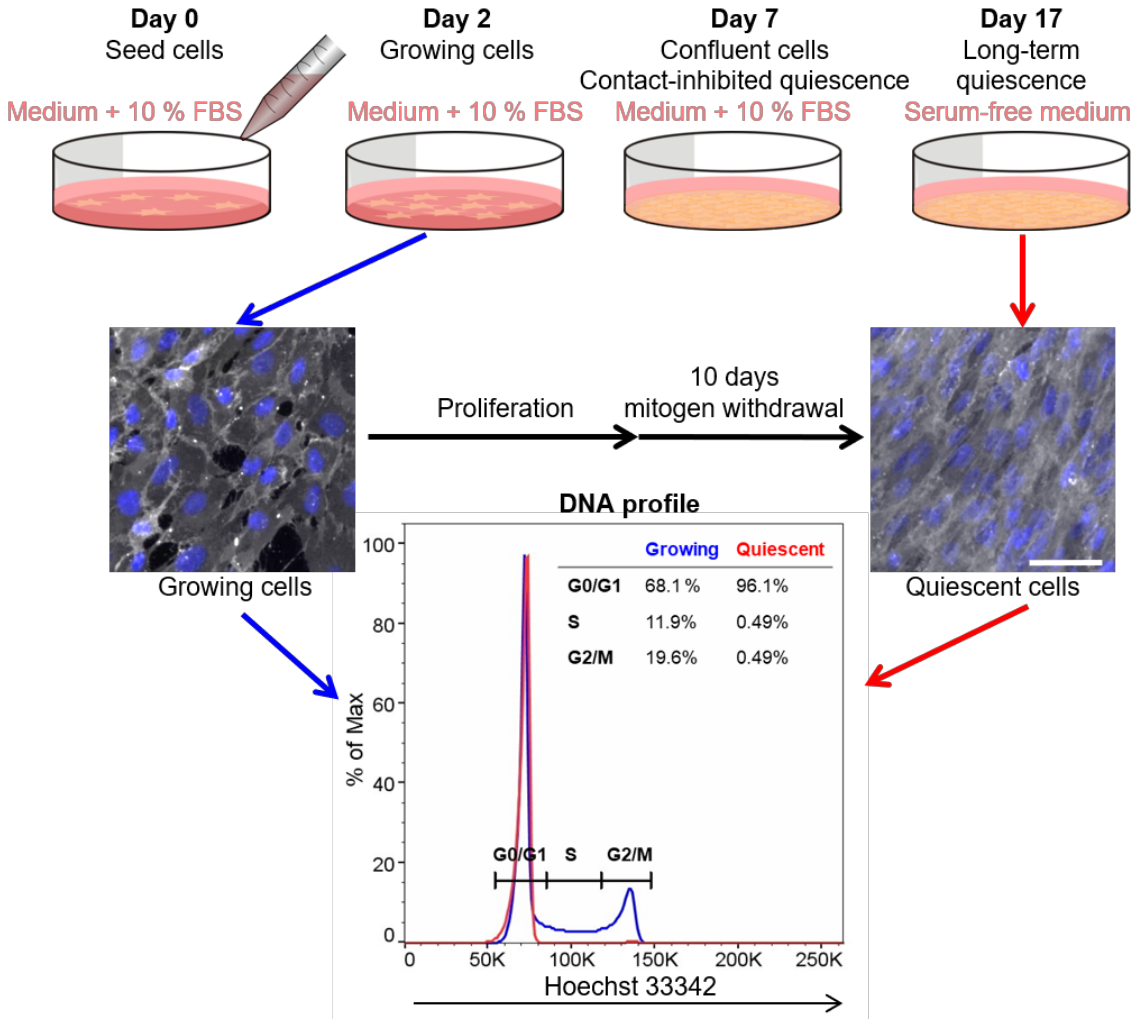

Figure 1: Induction of long-term quiescence, Bar, 50 μm.

3.3 Inhibiting endocytosis during cellular quiescence

Endocytosis can be inhibited by gene ablation, RNA interference (RNAi), overexpression of dominant-negative proteins, protein relocation or addition of small compounds inhibitors. Because of the many entry routes into cells, endocytic pathways cannot be all blocked at once - a perturbation that would be highly toxic to most, if not all, cells anyway. To date, only CME, macropinocytosis, CLIC/GEEC, FEME and Dynamin-dependent endocytosis (which includes CME and other pathways such as FEME) can be inhibited with some specificity. Owing to the difficutly of transfecting and expressing DNA plasmids in quiescent cells, we chose to present the inhibition of CME using AP2 RNAi and Pitstop 2 and blockage of macropinocytosis and Dynamin-mediated endocytosis using small compound inhibitors.

3.3.1 CME inhibition by RNA interference

Growing cells:

1. Six hours prior to transfection, seed growing cells at 6.9 x 10^3 cells/cm^2 in 96 well plates.
2. For each well, dilute 0.169 μL of Lipofectamine RNAiMAX transfection reagent in 4.831 μL OptiMEM, and 0.0675 μL of μ2-adaptin siRNA in 4.9325 μL OptiMEM, incubate 5 min at room temperature.
3. Mix diluted RNAiMAX with diluted siRNA and incubate for 20min at room temperature.
4. Add 10 μL transfection mix to each well containing 100 μl growth medium.

5. Repeat the transfection 24 hours after step 4.
6. Change the medium after 48 hours.
7. Use the cells 72 hours after step 4.

Quiescent cells:

1. Five days prior to transfection, seed growing cells at 1.4 x 10^4 cells/cm^2 in 96 well plates. (*see* **Note 22**).
2. For each well, dilute 0.85 μL of Lipofectamine RNAiMAX Transfection Reagent in 4.15 μL OptiMEM and 0.1 μL of μ2-adaptin siRNA in 4.9 μL OptiMEM, incubate 5 min at room temperature.
3. Mix diluted RNAiMAX with diluted siRNA and incubate for 20 min at room temperature.
4. Add 10 μL transfection mix to each well containing 100 μl growth medium.
5. Change the medium (full serum) after 24 hours
6. Repeat the transfection 48 hours after step 4.
7. Change the medium to serum-free 10 days after Step 1
8. Change the medium (serum-free) every 48 hours.
9. Use the cells ~12 days after step 4.

3.3.2 CME inhibition by Pitstop 2

Using the cell seeding procedure detailed in 3.1 and 3.2, treat growing and quiescent cell cultures as follow:

1. Dilute Pitstop 2 to 30 μM into the respective culture media.
2. Replace the culture media with mix from Step 1 and incubate at 37 °C for the appropriate duration (a minimum of 10 min and maximum of 4 hours is recommended) prior to the endocytic assays.

3.3.3 Dynamin inhibition by small inhibitors:

Dynamin is inhibited in cells by several small compound inhibitors at the following indicative working concentrations: Dyngo-4a, 4 to 10 μM (McCluskey et al. 2013), Chlorpromazine 18 μM (Daniel et al. 2015); dynole 34-2 10 μM (Hill et al. 2009) (*see* **Note 23**); Indole 24, 2 to 5 μM (Gordon et al. 2013); Quinone 45, 50 μM (MacGregor et al. 2014); Pyrimidyn 7, 10 to 30 μM (McGeachie et al. 2013); MitMAB, 30 μM (Quan et al. 2007)[], Aminopyrimidine, 10 to 50 μM (Odell et al. 2017), or Dynasore, 80 μM (Macia et al. 2006) (*see* **Note 24**). It is good practice to use at least two independent inhibitors to limit off target effects (*see* **Note 25**). Inhibiting Dynamin has a broad effect on endocytosis, consistent with its function in several endocytic pathways (including CME and FEME).

Using the cell seeding procedure detailed in 3.1 and 3.2, treat growing and quiescent cell cultures as follow:

1. Dilute the inhibitors to the appropriate concentration into serum-free medium (for both growing and quiescent cells). (*see* **Note 26**).
2. Wash cells in serum-free medium.
3. Replace the culture media with mixes from Step 1 and incubate at 37 °C for the appropriate duration (a minimum of 10 min and maximum of 4 hours is recommended) prior to the endocytic assays.

3.3.4 Macropinocytosis inhibition by small inhibitors:

Micropinocytosis (fluid-phase uptake) and macropinocytosis are inhibited by Na^+/H^+ exchange inhibitor ethyl-isopropyl amiloride (EIPA) at 10 to 25 μM (West et al. 1989; Hewlett et al. 1994) or by Rottlerin at 2-10 μM (Sarkar et al. 2005).

Using the cell seeding procedure detailed in 3.1 and 3.2, treat growing and quiescent cell cultures as follow:

1. Dilute the inhibitors to the appropriate concentration into the respective culture media.
2. Replace the culture media with mixes from Step 1 and incubate at 37 °C for the appropriate duration (a minimum of 10 min and maximum of 4 hours is recommended) prior to the endocytic assays.

3.4. Endocytic assays in quiescent cells.

Endocytosis of receptors can be measured either by the intracellular entry of antibody recognizing their ectodomains (antibody feeding assay) or by the uptake of their ligands. For CME, we recommend fluorescently-labelled transferrin (50-200 μg/ml) and LDL (5-15 μg/ml), or anti-TfR antibody suitable for feeding assay (0.1 to 10 μg/ml); for Dynamin-mediated endocytosis, fluorescently-labelled EGF (50 ng/ml) or anti-EGFR antibody suitable for feeding assay (0.1 to 10 μg/ml, together with 50 to 100 ng/ml unlabelled EGF); for micropinocytosis, Lucifer yellow (5 mg/mL), and for macropinocytosis, fluorescently-labelled Dextrans (0.5 to 10 mg/mL depending on size and fixation) and fluorescently-labelled BSA or DQ-BSA (100 mg/mL) (*see* **Note 27**).

3.4.1 Uptake of fluorescently-tagged fixable ligands.

For fluorescently-tagged Tf, LDL, EGF, that can be fixed by 4% PFA, do as follows:

Cells seeded on glass-bottom microplates should be prepared according to 3.1, 3.2 and 3.3, as appropriate.

1. Pre-warm (37 °C for 1h) ligand uptake assay (LUA) medium (*see* **Note 28**).
2. Dilute fluorescently-tagged ligand to the desired concentration in warm LUA medium (*see* **Note 29**).
3. Take cells out of the incubator, swiftly aspirate culture medium and replace it with pre-warmed LUA medium containing ligand, return the cells to the 37 °C incubator and start a timer (*see* **Note 30**).
4. After desired time has elapsed, remove the samples form the incubator and place them on a water-ice tray (*see* **Note 31**).
5. Aspirate LUA medium and wash the samples two times ice-cold PBS^{++}
6. Wash the samples two times (2 min each) with Stripping Buffer 1 (*see* **Note 32**).
7. Wash the cells three times with ice-cold PBS^{++} (*see* **Note 33**).
8. Add ice-cold fixative solution (4% PFA in PBS) and incubate on ice for 5 min and another 15 min at room temperature (*see* **Note 34**).
9. Wash the fixed cells three times with PBS containing 50 mM NH_4Cl (*see* **Note 35**).
10. Wash the samples three times with PBS and immunostain or store at 4 °C, as required (*see* **3.5**).

3.4.2 Uptake of fluorescently-tagged non-fixable ligands.

For fluorescently-tagged Dextrans, Lucifer Yellow and DQ-BSA, that cannot be fixed, do as follow:

Cells seeded on glass-bottom microplates should be prepared according to 3.1, 3.2 and 3.3, as apropriated.

1. Pre-warm (37 °C for 1h) ligand uptake assay medium (*see* **Note 28**).
2. Dilute fluorescently-tagged ligand to the desired concentration in warm ligand uptake assay (LUA) medium. (*see* **Note 29**).
3. Take cells out of the incubator, swiftly aspirate culture medium and replace it with pre-warmed LUA medium containing ligand, return the samples to the 37 °C incubator and start a timer (*see* **Note 30**).
4. 20 min before the end of the incubation time, add Hoechst 33342 (final concentration 2.5 μg/mL) and return samples to 37 °C. (*see* **Note 36**).
5. After desired time has elapsed, remove the samples form the incubator and place them on a water-ice tray,

aspirate assay medium and wash the samples 5 times with ice-cold PBS^{++} (*see* **Note 31**).

6. Exchange PBS to Imaging Medium and image the cells imediately (*see* **Note 37**).

3.4.3 Antibody feeding assays

Cells seeded on glass-bottom microplates should be prepared according to 3.1, 3.2 and 3.3, as appropriate.

1. Pre-warm (37 °C for 1h) antibody uptake assay medium (*see* **Note 28**).
2. Dilute antibodies to the desired concentration (for example, 5 *μ*g/ml for an antibody against the ectodomain of EGFR) in LUA Medium (*see* **Note 29**).
3. Take cells out of the incubator, swiftly aspirate culture medium and replace it with pre-warmed assay medium containing antibodies, return the cells to the 37 °C incubator and start a timer. (*see* **Note 30**).
4. After the desired time has elapsed, remove the samples from the incubator and place them on a water-ice tray.
5. Aspirate LUA medium and wash the samples three times with ice-cold PBS^{++} (*see* **Note 31**).
6. Wash the cells three times with Stripping Buffer 2 for 2 min (*see* **Note 38**).
7. Wash the cells three times with ice-cold PBS^{++} (*see* **Note 33**).
8. Add ice-cold fixative solution (4% PFA in PBS) and incubate on ice for 5 min and another 15 min at room temperature (*see* **Note 34**).
9. Wash the fixed cells three times with PBS containing 50 mM NH_4Cl (*see* **Note 35**).
10. Wash the samples three times with PBS and immunostain or store at 4 °C, as required (*see* **3.5**).

3.4.4 Cell surface receptor labeling

Correcting ligand/antibody uptake measurements with cell surface receptor availability is required to normalise for receptor abundance between growing and quiescent cells (a ligand might be less internalised during G0 because the cell surface levels of its receptor are decreased, instead of because the endocytic pathway is down-regulated).

Cells seeded on glass-bottom microplates should be prepared according to 3.1, 3.2 and 3.3, as appropriate.

1. remove the samples from the incubator and place them on a water-ice tray. (*see* **Note 39**).
2. Wash the cells three times with ice-cold PBS^{++} (*see* **Note 39**).
3. Keep cells on the water-ice tray and incubate them with Imaging Medium containing 1% BSA and the primary antobdies at the desired concentrations.
4. Incubate the samples for 90 min on a water-ice tray in a cold room (*see* **Note 39**).
5. Wash the cells three times with ice-cold PBS^{++} (*see* **Note 39**).
6. Add ice-cold fixative solution (4% PFA in PBS) and incubate on ice for 5 min and another 15 min at room temperature (*see* **Note 34**).
7. Wash the fixed cells three times with PBS containing 50 mM NH_4Cl (*see* **Note 35**).
8. Wash the samples three times with PBS and immunostain or store at 4 °C, as required (*see* **3.5**).

3.5 Fixation and immunofluorescence labeling

1. Wash the samples three times with PBS.
2. Incubate the samples with blocking buffer containing 5% BSA and 0.1% Saponin for 30 min at room temperature. (*see* **Note 40**).
3. Remove blocking buffer and incubate the cells with the relevant primary antibodies diluted in PBS containing 5% BSA and 0.1% Saponin for 90 min at room temperature or overnight at 4 °C.

4. Wash samples three times with PBS containing 0.1% Saponin.
5. Incubate cells with the relevant secondary antibodies and DAPI (2 μg/mL) diluted in PBS containing 5% BSA and 0.1% Saponin for 45 min in the dark, at room temperature (*see* **Note 41**).
6. Wash samples three times (5 min incubations) with PBS containing 0.1% Saponin.
7. Wash samples twice with PBS and twice with milliQ water.
8. Exchange the water for antifading mounting solution (containing Mowiol and DABCO or equivalent, 50-100μl per well).
9. Image immediately or incubate the samples overnight at room temperature before long-term storage at 4°C.

3.6 Image acquisition by high-throughput automated widefield microscopy

The protocol below is for image acquisition of glass-bottom 96 well plates on an ImageXpress Micro XL widefield High Content Screening System (Molecular Devices) or equivalent. The protocol can be adapted for manual image acquisition, regular microscopy slides, confocal or super-resolution microscopy, as appropriate.

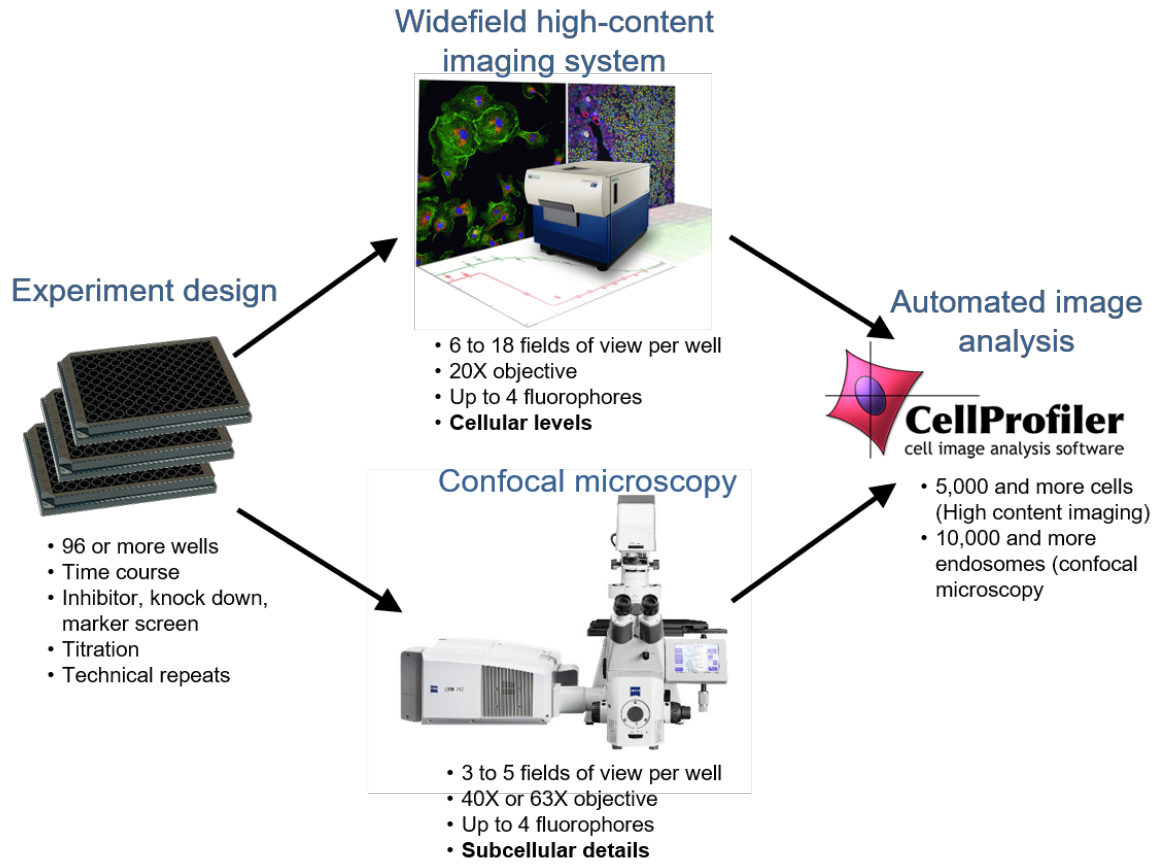

Figure 2: Adaptations for analysis of high-throughput experiments in 96-well plates

1. Prior to imaging, calibrate plates to allow for 96-well plate and bottom autofocus set up (**Figure 3**, step 1)
2. Select objective (*see* **Note 42**) (**Figure 3**, step 2)
3. Select the number of locations and sites to be imaged (**Figure 3**, step 3)

4. Set up the acquisition loop for each image (**Figure 3**, step 4):
    i. Select laser-based focusing on plate and well bottom for each image.
    ii. Select wavelength channels for excitation and emission appropriate for your fluorophore dyes.
    iii. Select the channel serving as focus offset for each other channel.
    iv. Determine the image-based focus and exposure times for each channel.
5. Apply a focus journal after each image acquisition to account for unevenness in plate design and focus planes (**Figure 3**, step 5) (*see* **Note 43**).
6. Run the image acquisition for the wells selected.

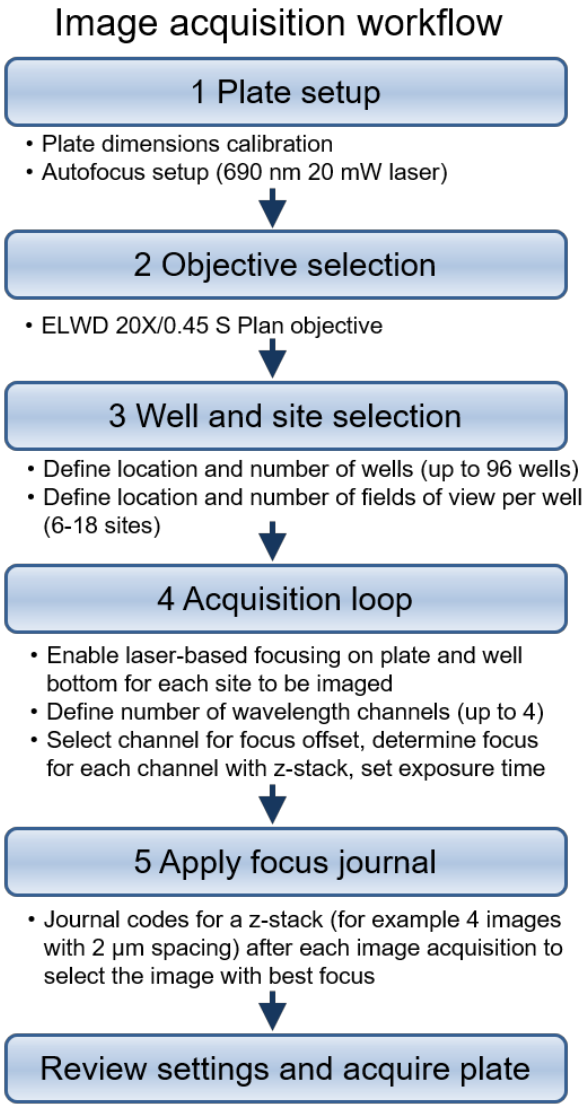

Figure 3: Plate setup and image acquisition

3.7 Automated image analysis

We recommend analyzing the images acquired by confocal or high throughput microscopy with the open source software CellProfiler 2.2.0 (Carpenter *et al.*, 2006; Lamprecht *et al.*, 2007). Alternative analysis software or routines can be used instead. Import image sets (one image set consist of up to four separate images, one for each wavelength) into CellProfiler together with metadata information about experiment name, well and site number and wavelength channel extracted with regular expressions.

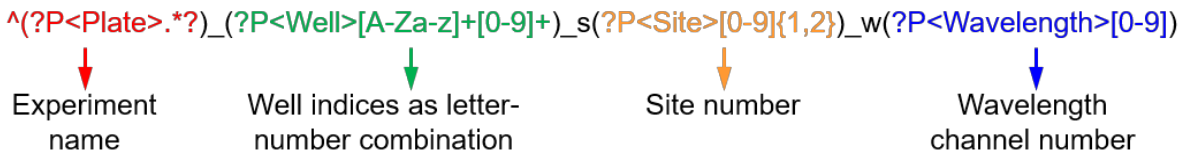

Figure 4: Regular expression to extract metadata information from image file names in CellProfiler

3.7.1 Cell segmentation and endosome identification

The workflow of a CellProfiler pipeline segmenting cells and endosomes is shown in **Figure 5**.

1. Treat the greyscale images for each wavelength channel separately.
2. Calculate an illumination function and background-subtract it from the raw images to account for uneven illumination during image acquisition (**Figure 5**, step 1).
3. Rescale illumination-corrected images (on a scale of 0-1), so that faint signals are visible for object identification (**Figure 5**, step 2).
4. On rescaled images, identify nuclei labeled with DAPI or Hoechst 33342 as primary objects (**Figure 5**, step 3).
5. Identify cell bodies labeled with a cytoplasmic marker (such as GAPDH or F-actin) as secondary objects emanating from a primary object (**Figure 5**, step 4).
6. Create a mask on the identified cell bodies to eliminate areas not occupied by cells from further analysis (**Figure 5**, step 5).
7. Within the mask, enhance speckles (which are small circular areas of increased intensity compared to their immediate environment) to distinguish them from background haze. Additionally, this step eliminates large areas of signal caused by antibody aggregation or surface-bound antibody that was not efficiently stripped (**Figure 5**, step 6).
8. Use the speckle-enhanced images to identify endosomes as puncta of a defined pixel size (usually 4-15 pixels diameter) (**Figure 5**, step 7).
9. Measure mean intensity and total area of puncta identified in illumination-corrected images created in step 2 (**Figure 5,** step 8).
10. For quantitation, subtract mean fluorescence of puncta per image by the mean fluorescence of cells per image in blank images (cell not subjected to ligand uptake but else treated in the same way). Finally, multiply by the total area of puncta per cells to get the sum of the ligand internalized into endosomes.

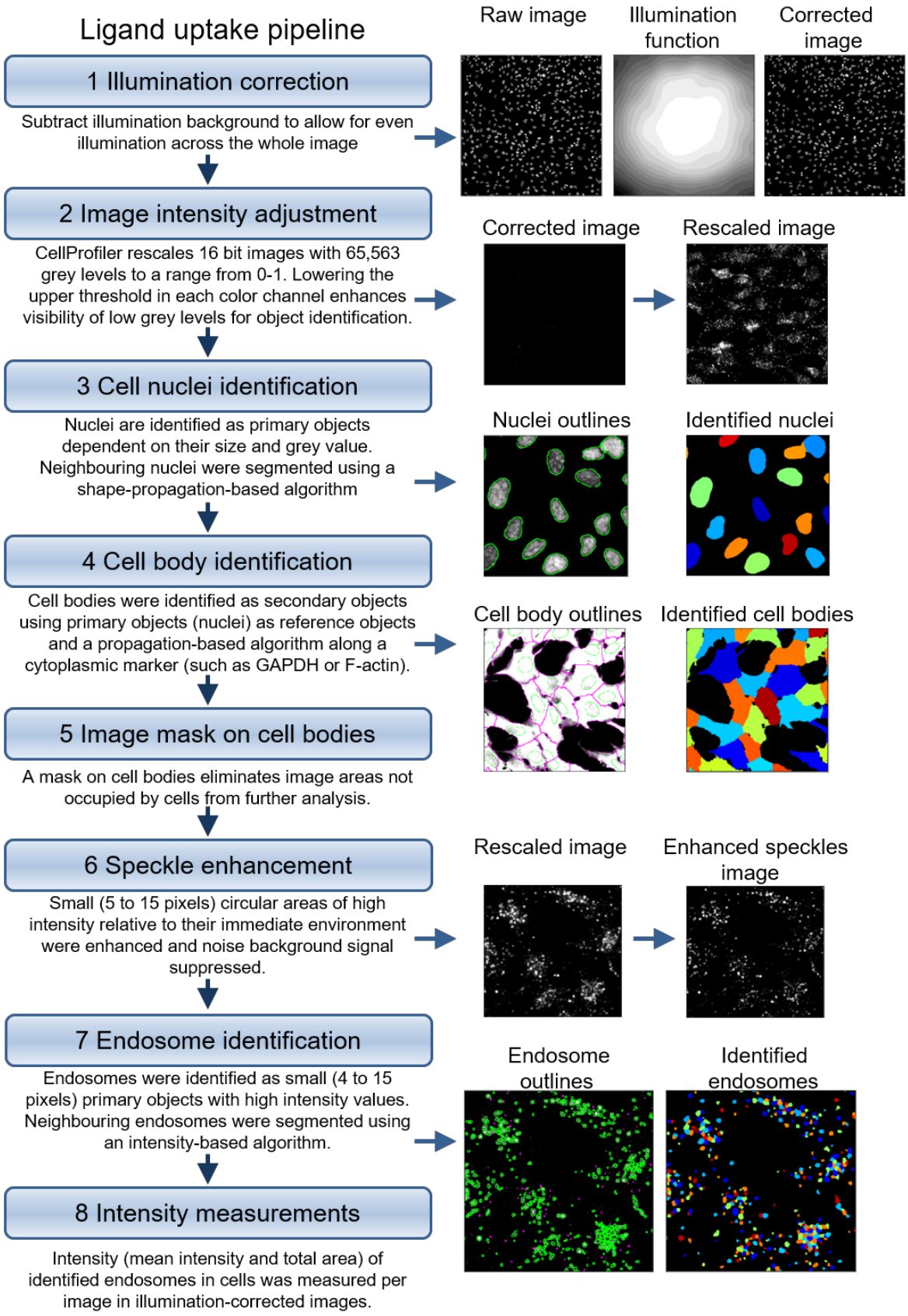

Figure 5: CellProfiler workflow to segment cells and identify internalized ligand or receptor puncta.

3.7.2 Object-based colocalization analysis

The workflow of a CellProfiler pipeline identifying endosome colocalization is shown in **Figure 6**. This analysis is only suitable for images acquired by confocal microscopy.

1. Correct (illumination correction) and rescale images, enhance speckles and identify endosomes as in 3.7.1.
2. Shrink identified puncta either to a central pixel or by a specified number of pixels, according to the desired analysis stringency (**Figure 6**, step 3).
3. Identify the colocalisation of shrunk puncta in different channels (images) by relating overlapping objects in a child-parent relationship and filter children with a parent or *vice versa* (**Figure 6**, step 4).
4. To relate the intensities measured to the original-size endosomes, relate the shrunken puncta with their parent (or child) back to the puncta identified initially (**Figure 6**, step 5).
5. Measure the percentage of colocalization by relating the total intensity of colocalized signals and total amount of identified puncta in illumination-corrected images

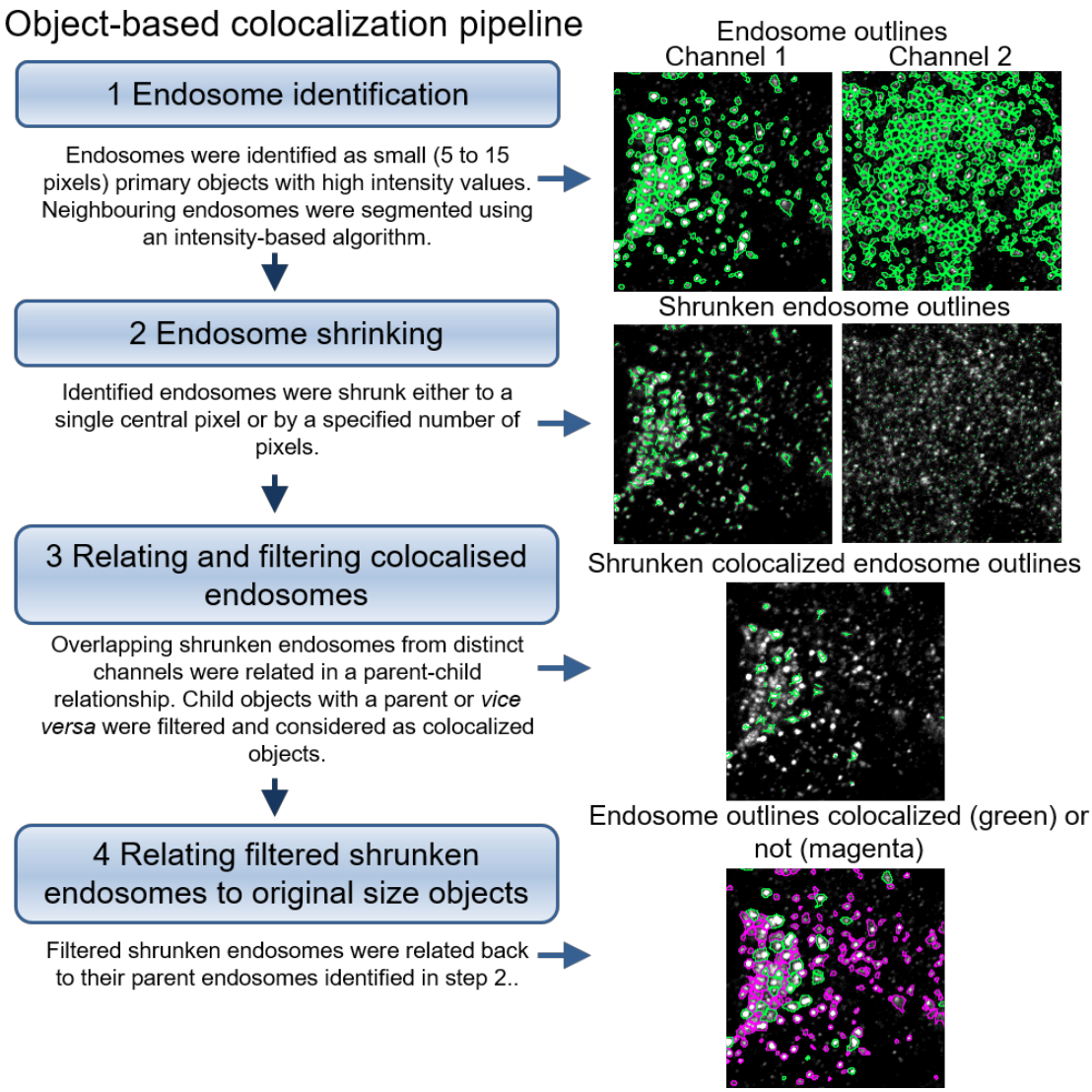

Figure 6: Object-based colocalization using CellProfiler.

3.8 Statistical analysis

An advantage of high content imaging is the measurement of high numbers (multiple thousands) of cells, giving robust statistics.

1. Test for Gaussian distribution of the data using D'Agostino & Pearson omnibus normality test or equivalent.

2. for samples that follow Gaussian distribution: test for statistical significance using Student's or Welch's unpaired two-tailed *t*-test (two sample groups), one-way ANOVA and Dunett's test for multiple comparisons (more than two sample groups) or two-way ANOVA with Tukey's test for multiple comparisons (more than two sample groups with multiple parameters per group), as appropriate.

3. for samples that do not follow Gaussian distribution: test for statistical significance using Mann-Whitney *U*-test (two-sample groups), Kruskal Wallis test with Dunn's multiple comparison (more than two sample groups) or Friedman test with Dunn's test for multiple comparisons (more than two sample groups with multiple parameters per group), as appropriate.

3.9 Representative result

Figure shows EGF uptake (50 ng/mL AlexaFluour647-EGF for 15 min at 37°C) into growing and quiescent cells. Approximately 400,000 and 60,000 intracellular EGF puncta were identified and quantified, in 10,000 and 19,000 growing and quiescent cells respectively, corresponding to an average of 40 puncta per growing and 3 puncta per quiescent cell.

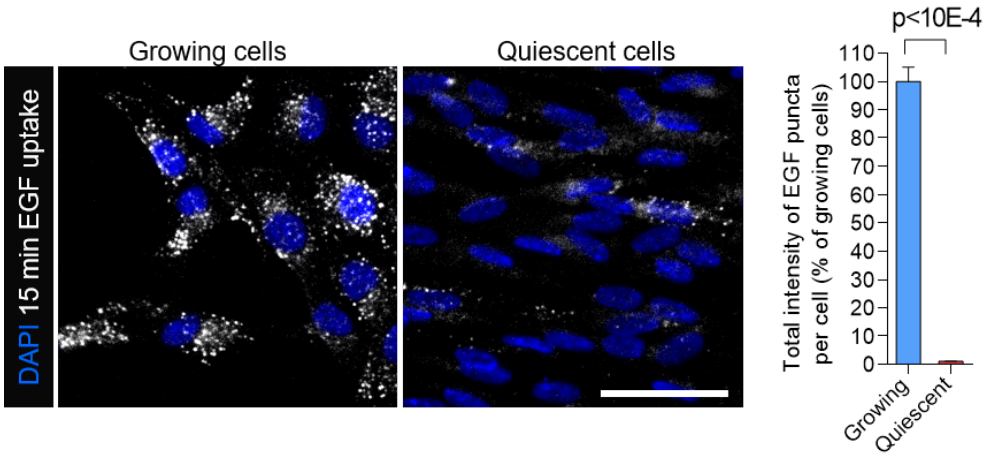

Figure 7: Quantification of 15 min EGF uptake in growing and quiescent cells. Scale bar: 50µm.

4. Notes

1. A wide variety of cells may be used as long as they maintain cell cycle exit upon contact-inhibition (it is not the case for commonly used tumor-derived cell lines). The methods described here use human normal, diploid hTERT-RPE1 cells, but are easily adapted for other primary or hTERT-immortalized cell types.

2. Growing cells are cultured in full serum-containing medium (*e.g.* 10% FBS or equivalent)

3. Quiescent cells survive for long periods of time (months) in growth factor-free medium (i.e. serum-free) containing regular levels of amino acids, glucose and other supplements.

4. Detaching cells with trypsin-based solutions is possible although less desirable as it shaves cells from a significant proportion of their cell surface receptors.

5. The protocol can be adapted to any other size and type of tissue culture containers.

6. Presence of Ca^{2+} and Mg^{2+} is required for cell adhesion and survival until fixation.

7. Other chemical inhibitions of CME such as hypertonic shock (0.45 M sucrose), cytosol acidification (Sandvig 1987), potassium depletion, monodansylcadaverine or phenylarsine oxide (Schlegel et al. 1982; Larkin et al. 1983; Gibson et al. 1989; Heuser and Anderson 1989; Wang et al. 1993), even though widely used in the literature, are not recommended as they affect clathrin-independent endocytosis, including FEME, as well (Boucrot et al. 2015).

8. Chlorpromazine was initially believed to be a Clathrin and/or AP2 inhibitor (Wang et al. 1993), but was recently found to inhibit Dynamin instead (Daniel et al. 2015).

9. RNA interference of AP2 is preferable to that of Clathrin as the latter has many functions beside endocytosis (Brodsky et al. 2014). Gene editing using CRISPR/Cas9 is also possible.

10. The choice of fluorophore depends on the sensitivity of the microscope used. We found that Alexa647-labelled ligands have the highest signal-to-noise ratio.

11. Antibodies suitable for feeding assays must bind to the extracellular parts of the receptor of interest.

12. Whilst both intercalating dyes stain DNA in a stoichiometric manner, Hoechst 33342 is cell-permable (and thus can be used on live cells), whereas DAPI is not.

13. The protocol can be easily adapted to any kind of widefield, confocal or super-resolution microscopes, as appropriated.

14. We found that passaging primary and hTERT-immortalized cells before they reach such confluency ensures exponential growth whilst minimizing sub-populations of quiescent cells (happening when patches of cells become confluent).

15. We typically passage growing cells every 2 days (highest seeding density provided). Seeding cells at the lowest density will allow for ~ 3 days until the next passage.

16. Growing cells need full-serum medium.

17. We found that seeding cells at this density ensures ordinate formation of homogeneous monolayers.

18. Cells must be grown in presence of growth factor-containing (full serum) medium until tight monolayers are formed.

19. The formation of tight and well-organized monolayers (i.e. where cells are oriented in the same direction) are important to induce deep quiescence.

20. Once monolayers are formed, cells can be maintained in growth factor-free (serum-free) medium. Primary cells will enter apoptosis if growth factors are removed prior to cell confluency.

21. We found that 10 days growth factor removal after monolayer establishment is enough to induce deep quiescence.

22. We found that siRNA oligos transfection and RNA interference is more efficient whilst the cells are entering quiescent. Once in G0, protein levels of RNAi targets remain depressed for long periods (multiple days).

23. Dynole 32-1 is negative control compound for Dynole 34-1 (Hill et al. 2009).

24. Although not as potent or specific as the ones selected, other Dynamin inhibitors such as OctMAB, Pro-Myristic Acid, Rhodadyn C10 or Iminodyn-22 (Quan et al. 2007; Hill et al. 2009; Robertson et al. 2012) can be used as well.

25. It is best practice to use small inhibitors against different domains of Dynamin (e.g. Dyngo-4a or Dynole 34-2 targeting the G-domain and MitMAB, OctAB or Pro-Myristic Acid targeting the PH domain).

26. Many small compound inhibitors are hydrophobic and quenched by serum (mostly albumin presented therein), thereby reducing their active concentration.

27. Lucifer yellow is a fluid-phase marker. Dextrans of various sizes (from 3,000 to 2,000,000+ kDa) can be used to discriminate between small micropinosomes and large macropinosomes. DQ-BSA only fluoresces when it reaches degradative endolysosomes, thereby ensuring the uptake of the probe.

28. Pre-warming ligand/antibody uptake medium is required to maintain the temperature of the cells as close to 37 °C as possible throughout the assay.

29. Small compound inhibitors must be present with the ligands for the relevant samples.

30. Incubations times can vary from 1 min to 60 min, as required. To measure endocytic rates (expressed as amount of ligand per unit of time), several lengths of incubations must be measured.

31. The use of cold temperatures at the end of the assay is appropriate as the cells will be fixed shortly after. Adding ice-cold PBS^{++} stops any trafficking within seconds. Using ice + water mix to cool the plates/dishes during the subsequent steps ensures a better temperature exchange and cooling than using ice only.

32. Washes with a mildly acidic stripping buffer ('Stripping buffer 1', pH 5.5) remove cell surface ligands that were not internalized after incubation (internalized ligands are protected within endocytic carriers or endosomes).

33. Washes with PBS are required for raising the pH back to ~7.4 after washes with stripping buffers.

34. Cold fixation is required to avoid that endocytosis resumes unwittingly.

35. Washes with 50 mM NH_4Cl in PBS are required to inactivate any residual reactive PFA.

36. Staining DNA with cell-permeable Hoechst 33342 is important for automated cell identification (section 3.7).

37. Imaging should be done at 37 °C if image acquisition can be done within 10 min. Do the imaging at 4°C otherwise (to slow down endosomal recycling and degradation of the ligands).

38. Washes with an acidic stripping buffer ('Striping buffer 2', pH 2) remove cell surface antibodies that were not internalized after incubation. Note that cell surface stripping of antibodies requires lower pH than that of endocytic ligands.

39. Low temperature is required for cell surface staining to stop receptor trafficking.

40. We typically use Saponin to permeabilize cells but other means (Triton X-100, cold methanol) can be used as well.

41. Fluorescently-labeled secondary antibodies towards the species of internalized antibodies must be included in the immunostaining procedure (*e.g.* AlexaFluor-488 coupled Goat anti-Rabbit secondary antibodies to label Rabbit anti-EGFR antibodies internalized during the feeding assay). Counterstaining of protein(s) of interest, DNA (using DAPI or DRAQ5) and/or actin cytoskeleton (phalloidin) using other fluorophores than those coupled on the internalised ligand can be considered.

42. 20x objectives are typically sufficient to identify single endosomes whilst acquiring enough cells per field of view

43. The journal encoded a z-stack (e.g. 4 images with 2 µm spacing, set manually) from which the image with the best focus is saved as final acquisition.

Acknowledgement

C.H. was supported by a studentship from the British Heart Foundation (FS/14/20/30681). K.McG. was supported by the Biotechnology and Biological Sciences Research Council (BBSRC) and a UL-Health Research Institute Seed Award. E.B. was a Biotechnology and Biological Sciences Research Council (BBSRC) David Phillips Research Fellow and a Lister Institute Research Fellow. Part of this work was supported by a BBSRC grant (BB/R0155X/1) and a Birkbeck Wellcome Trust Institutional Strategic Support Fund (ISSF) grant to E.B.

References

Augenlicht LH, Baserga R (1974) Changes in the G0 state of WI-38 fibroblasts at different times after confluence. Exp Cell Res 89:255–262.

Benecke BJ, Ben-Ze'ev A, Penman S (1978) The control of mRNA production, translation and turnover in suspended and reattached anchorage-dependent fibroblasts. Cell 14:931–9

Bodnar AG, Ouellette M, Frolkis M, et al (1998) Extension of life-span by introduction of telomerase into normal human cells. Science (80-) 279:349–352.

Boucrot E, Ferreira APA, Almeida-Souza L, et al (2015) Endophilin marks and controls a clathrin-independent endocytic pathway. Nature 517:460–465.

Brodsky FM, Thomas Sosa R, Ybe JA, O'Halloran TJ (2014) Unconventional functions for clathrin, ESCRTs, and other endocytic regulators in the cytoskeleton, cell cycle, nucleus, and beyond: Links to human disease. Cold Spring Harb Perspect Biol 6:.

Coller H a, Sang L, Roberts JM (2006) A new description of cellular quiescence. PLoS Biol 4:e83.

Crissman HA, Darzynkiewlcz Z, Tobey RA, Steinkamp JA (1985) Normal and Perturbed Chinese Hamster Ovary Cells: Correlation of DNA, RNA, and Protein Content By Flow Cytometry. J Cell Biol 101:141–147

Daignan-Fornier B, Sagot I (2011) Proliferation/quiescence: the controversial "aller-retour". Cell Div 6:10.

Daniel JA, Chau N, Abdel-Hamid MK, et al (2015) Phenothiazine-Derived Antipsychotic Drugs Inhibit Dynamin and Clathrin-Mediated Endocytosis. Traffic 16:635–654.

Doherty GJ, McMahon HT (2009) Mechanisms of endocytosis. Annu Rev Biochem 78:857–902.

Ferreira APA, Boucrot E (2018) Mechanisms of Carrier Formation during Clathrin-Independent Endocytosis. Trends Cell Biol 28:188–200.

Fuge EK, Braun EL, Werner-Washburne M (1994) Protein synthesis in long-term stationary-phase cultures of Saccharomyces cerevisiae. J Bacteriol 176:5802–5813.

Gibson AE, Noel RJ, Herlihy JT, Ward WF (1989) Phenylarsine oxide inhibition of endocytosis: Effects on asialofetuin internalization. Am J Physiol - Cell Physiol 257:.

Gookin S, Min M, Phadke H, et al (2017) A map of protein dynamics during cell-cycle progression and cell-cycle exit. PLoS Biol 15:e2003268.

Gordon CP, Venn-Brown B, Robertson MJ, et al (2013) Development of second-generation indole-based dynamin GTPase inhibitors. J Med Chem 56:46–59.

Gos M, Miloszewska J, Swoboda P, et al (2005) Cellular quiescence induced by contact inhibition or serum withdrawal in C3H10T1/2 cells. Cell Prolif 38:107–16.

Gray J V, Petsko GA, Johnston GC, et al (2004) ' ' Sleeping Beauty ' ': Quiescence in Saccharomyces cerevisiae.

Microbiol Mol Biol Rev 68:187–206.

Hanahan D, Weinberg RA (2011) Hallmarks of Cancer: The Next Generation. Cell 144:646–674.

Hemalatha A, Mayor S (2019) Recent advances in clathrin-independent endocytosis. F1000Research 8

Herman PK (2002) Stationary phase in yeast. Curr. Opin. Microbiol. 5:602–607

Heuser JE, Anderson RGW (1989) Hypertonic media inhibit receptor-mediated endocytosis by blocking clathrin-coated pit formation. J Cell Biol 108:389–400.

Hewlett LJ, Prescott AR, Watts C (1994) The coated pit and macropinocytic pathways serve distinct endosome populations. J Cell Biol 124:689–703

Hill TA, Gordon CP, McGeachie AB, et al (2009) Inhibition of dynamin mediated endocytosis by the Dynoles - Synthesis and functional activity of a family of indoles. J Med Chem 52:3762–3773.

Hinze C, Boucrot E (2018) Endocytosis in proliferating, quiescent and terminally differentiated cells. J Cell Sci 131:jcs216804.

Kaksonen M, Roux A (2018) Mechanisms of clathrin-mediated endocytosis. Nat Rev Mol Cell Biol 19:313–326.

Kogan I, Goldfinger N, Milyavsky M, et al (2006) hTERT-immortalized prostate epithelial and stromal-derived cells: An authentic in vitro model for differentiation and carcinogenesis. Cancer Res 66:3531–3540.

Laporte D, Salin B, Daignan-Fornier B, Sagot I (2008) Reversible cytoplasmic localization of the proteasome in quiescent yeast cells. Chemtracts 21:224–226.

Larkin JM, Brown MS, Goldstein JL, Anderson RGW (1983) Depletion of intracellular potassium arrests coated pit formation and receptor-mediated endocytosis in fibroblasts. Cell 33:273–285.

Lemons JMS, Feng X-J, Bennett BD, et al (2010) Quiescent fibroblasts exhibit high metabolic activity. PLoS Biol 8:e1000514.

MacGregor KA, Abdel-Hamid MK, Odell LR, et al (2014) Development of quinone analogues as dynamin GTPase inhibitors. Eur J Med Chem 85:191–206.

Macia E, Ehrlich M, Massol R, et al (2006) Dynasore, a cell-permeable inhibitor of dynamin. Dev Cell 10:839–50.

Maldonado-Báez L, Williamson C, Donaldson JG (2013) Clathrin-independent endocytosis: A cargo-centric view. Exp. Cell Res. 319:2759–2769

McCluskey A, Daniel JA, Hadzic G, et al (2013) Building a better dynasore: The dyngo compounds potently inhibit dynamin and endocytosis. Traffic 14:1272–1289.

McGeachie AB, Odell LR, Quan A, et al (2013) Pyrimidyn compounds: Dual-action small molecule pyrimidine-based dynamin inhibitors. ACS Chem Biol 8:1507–1518.

McMahon HT, Boucrot E (2011) Molecular mechanism and physiological functions of clathrin-mediated endocytosis. Nat Rev Mol Cell Biol 12:517–33.

Mettlen M, Chen P-H, Srinivasan S, et al (2018) Regulation of Clathrin-Mediated Endocytosis. Annu Rev Biochem 87:871–896.

Narayanaswamy R, Levy M, Tsechansky M, et al (2009) Widespread reorganization of metabolic enzymes into reversible assemblies upon nutrient starvation. Proc Natl Acad Sci U S A 106:10147–10152.

Odell LR, Abdel-Hamid MK, Hill TA, et al (2017) Pyrimidine-Based Inhibitors of Dynamin I GTPase Activity: Competitive Inhibition at the Pleckstrin Homology Domain. J Med Chem 60:349–361.

Owen TA, Cosenza SC, Soprano DR, Soprano KJ (1989) Evidence that stimulation of growth following long term density arrest of WI-38 cells proceeds via a pathway independent of protein kinase C and of cAMP-dependent protein kinase. Oncogene Res 4:137–47

Quan A, McGeachie AB, Keating DJ, et al (2007) Myristyl trimethyl ammonium bromide and octadecyl trimethyl ammonium bromide are surface-active small molecule dynamin inhibitors that block endocytosis mediated by dynamin I or dynamin II? Mol Pharmacol 72:1425–1439.

Renard HF, Johannes L, Morsomme P (2018) Increasing Diversity of Biological Membrane Fission Mechanisms.

Trends Cell Biol. 28:274–286

Robertson MJ, Hadzic G, Ambrus J, et al (2012) The Rhodadyns, a new class of small molecule inhibitors of dynamin gtpase activity. ACS Med Chem Lett 3:352–356.

Sagot I, Pinson B, Salin B, Daignan-Fornier B (2006) Actin bodies in yeast quiescent cells: An immediately available actin reserve? Mol Biol Cell 17:4645–4655.

Sandvig K (1987) Acidification of the cytosol inhibits endocytosis from coated pits. J Cell Biol 105:679–689.

Santos AJM, Boucrot E (2018) Probing endocytosis during the cell cycle with minimal experimental perturbation. In: Methods in Molecular Biology. Humana Press Inc., pp 23–35

Sarkar K, Kruhlak MJ, Erlandsen SL, Shaw S (2005) Selective inhibition by rottlerin of macropinocytosis in monocyte-derived dendritic cells. Immunology 116:513–524.

Schlegel R, Dickson RB, Willingham MC, Pastan IH (1982) Amantadine and dansylcadaverine inhibit vesicular stomatitis virus uptake and receptor-mediated endocytosis of α2-macroglobulin. Proc Natl Acad Sci U S A 79:2291–2295.

Schmid SL (2017) Reciprocal regulation of signaling and endocytosis: Implications for the evolving cancer cell. J Cell Biol 216:2623–2632.

Sherr CJ, DePinho RA (2000) Cellular senescence: Mitotic clock or culture shock? Cell 102:407–410

Sigismund S, Confalonieri S, Ciliberto A, et al (2012) Endocytosis and signaling: cell logistics shape the eukaryotic cell plan. Physiol Rev 92:273–366.

Sigismund S, Scita G (2018) The ‘endocytic matrix reloaded’ and its impact on the plasticity of migratory strategies. Curr. Opin. Cell Biol. 54:9–17

Soprano KJ (1994) WI-38 cell long-term quiescence model system: A valuable tool to study molecular events that regulate growth. J Cell Biochem 54:405–414.

Valentin M, Yang E (2008) Autophagy is activated, but is not required for the G0 function of BCL-2 or BCL-xL. Cell Cycle 7:2762–2768.

Wang LH, Rothberg KG, Anderson RGW (1993) Mis-assembly of clathrin lattices on endosomes reveals a regulatory switch for coated pit formation. J Cell Biol 123:1107–1117.

Wang X, Fujimaki K, Mitchell GC, et al (2017) Exit from quiescence displays a memory of cell growth and division. Nat Commun 8:321.

West MA, Bretscher MS, Watts C (1989) Distinct endocytotic pathways in epidermal growth factor-stimulated human carcinoma A431 cells. J Cell Biol 109:2731–9.

Yanez I, O’Farrell M (1989) Variation in the length of the lag phase following serum restimulation of mouse 3T3 cells. Cell Biol Int Rep 13:453–462.

Yusuf I, Fruman DA (2003) Regulation of quiescence in lymphocytes. Trends Immunol 24:380–386.